where W_d is the length scale (km) and R is the rain rate (mm/h) for debris. This is more conveniently expressed in terms of attenuation for determining the effective rain rate (R") in debris.:

$$W_d = 29.7^{\alpha/(\alpha - .34)} \; K^{[.34/(\alpha - .34)]} \; A^{-[.34/(\alpha - .34)]} \qquad (3.5\text{-}7)$$

$$W'_d = \text{minimum } (W_d, D_d) \qquad (3.5\text{-}8)$$

$$R'' = \left(\frac{A}{kW'_d}\right)^{1/\alpha} \qquad (3.5\text{-}9)$$

where R" is the effective rain rate for debris.

3.5.3 Probability of Exceeding an Attenuation Threshold

A simple approximation to the observed (Kansas) rain rate distribution produced by volume cells is an exponential distribution. The debris distribution function was nearly log-normal. The sum of these independent distributions was found to closely fit the empirical rain rate distributions for all climate regions. Thus:

$$P(r \geq R) = P_c(r \geq R) + P_d(r \geq R) \qquad (3.5\text{-}10)$$

$$= p_c(1 + D_c/W_c) \exp(-R'/R_c)$$

$$+ p_d(1 + D_d/W_d) \, \eta[(1/\sigma_d)[\ell n \, R'' - \ell n \, R_d)] \qquad (3.5\text{-}11)$$

where $P(r \geq R)$ is the probability of the observed rain rate r exceeding the specified rain rate R; $P_{c,d}(r \geq R)$ are the distribution functions for volume cells and debris, respectively; $p_{c,d}$ are the probabilities of a cell and debris, respectively; $R_{c,d}$ are the average rain rates in cells and debris, respectively; σ_d is the standard deviation of the logarithm of the rain rate; and η is the normal distribution function. Values for the parameters p_c, p_d, R_c, and σ_d have been tabulated for each of the Global Model rain climate regions (Crane-1982).

3.6 THE CCIR MODEL

The International Radio Consultative Committee, CCIR, adopted a procedure for the prediction of attenuation caused by rain at its XVth Plenary Assembly in Geneva in Febrary 1982 (CCIR-1982a). This result was preceeded by several years of intense deliberations by representatives of CCIR Study Group V from several nations. The procedure provided the basis for rain attenuation calculations required for international planning and coordination meetings, and Regional and World Administrative Radio Conferences.

The original CCIR procedure has undergone several modifications, including deliberations for the 1982 Conference Preparatory Meeting for RARC-83 for the Broadcasting Satellite Service (CCIR-1982b, CCIR-1982c), and the Study Group 5 Inputs for the XVIth Plenary Assembly, in Dubrovnik, Yugoslavia (CCIR-1985a, CCIR-1985b). The rain characterization and attenuation prediction procedures described in this handbook are the latest published versions, as provided in Reports 563-3 (CCIR-1986a), and 564-3 (CCIR-1986b), respectively, from the XVIth Plenary Assembly. Readers interested in tracing the evolution of the CCIR prediction procedure development process are referred to the earlier documents referenced above.

3.6.1 CCIR Rain Characterization

The first element of the CCIR Model involves a global map of fourteen rain climatic zones with associated rainfall intensity cumulative distributions for each region specified (CCIR-1986a). Average annual rain rates are given for exceedance times fro 0.001 to 1.0 percent. Figure 3.6-1 presents the global map of the CCIR rain climatic zones, ranging from A (light rains) to P (heavy rains). A more detailed map of the CCIR climatic zones for the continental United States and Canada is shown in Figure 3.6-2 (Ippolito, 1986). Table 3.6-1 lists the rain rate distributions for the fourteen rain climatic zones.

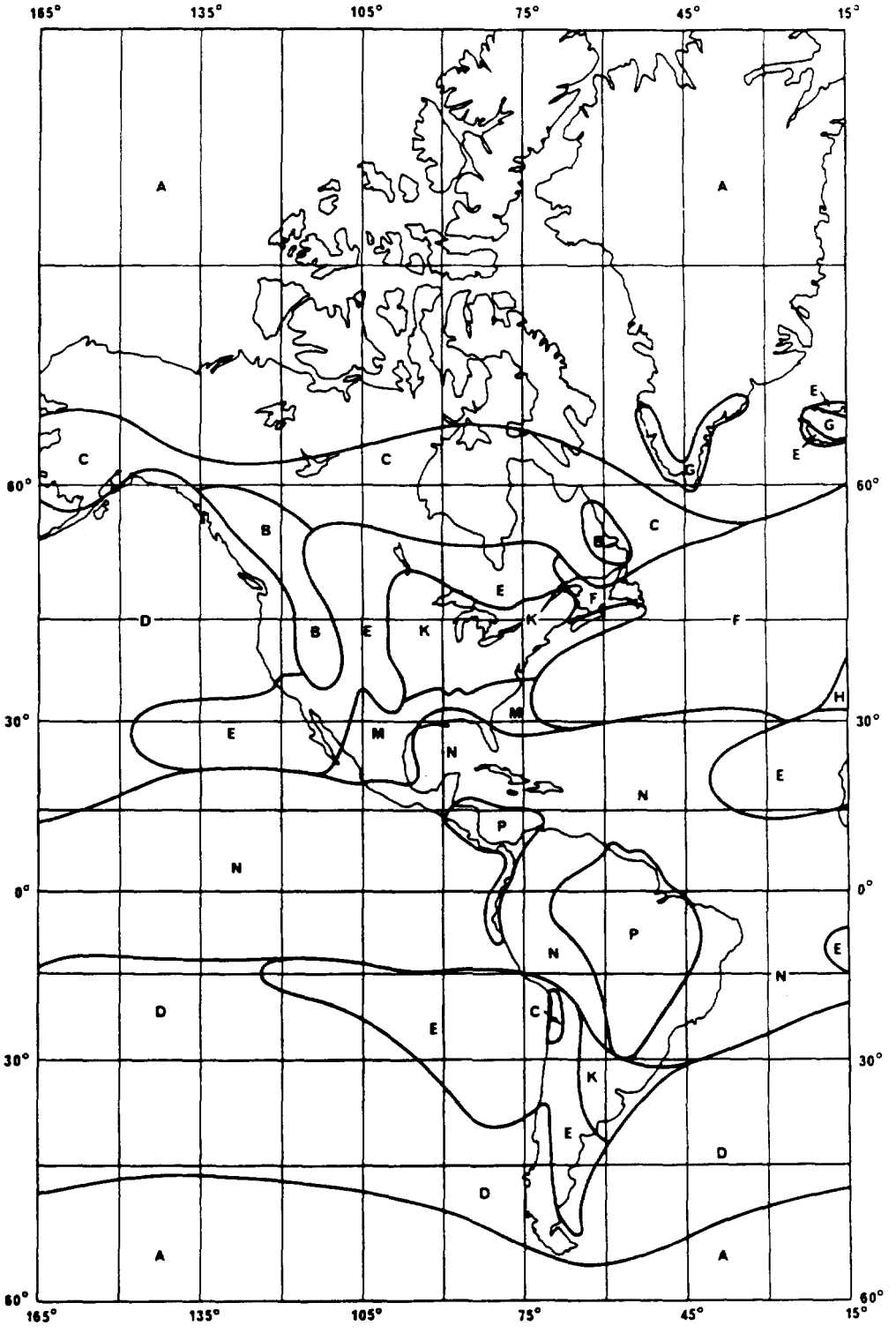

Figure 3.6-1. CCIR Rain Climate Zones (Sheet 1 of 3)

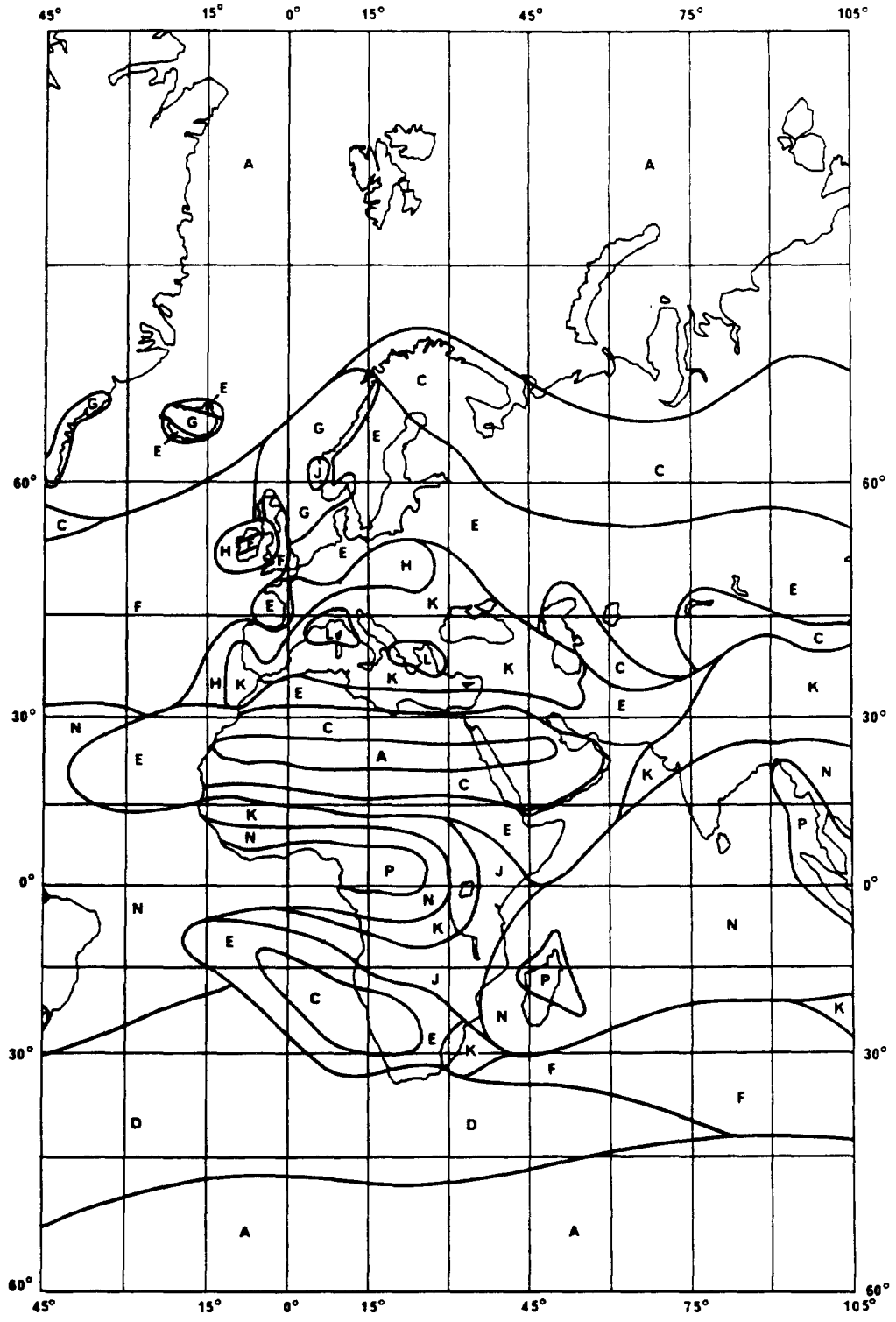

Figure 3.6-1. CCIR Rain Climate Zones (Sheet 2 of 3)

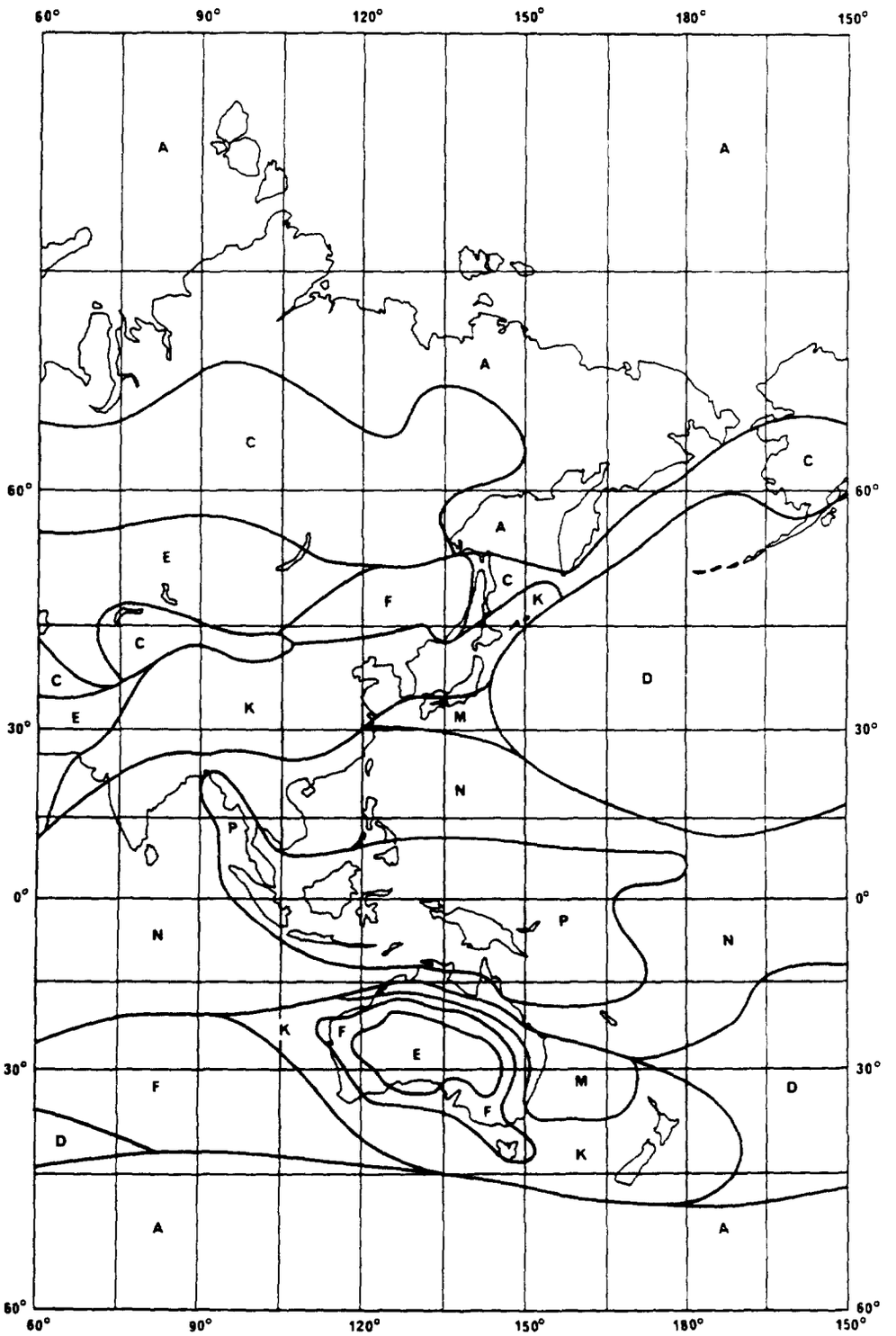

Figure 3.6-1. CCIR Rain Climate Zones (Sheet 3 of 3)

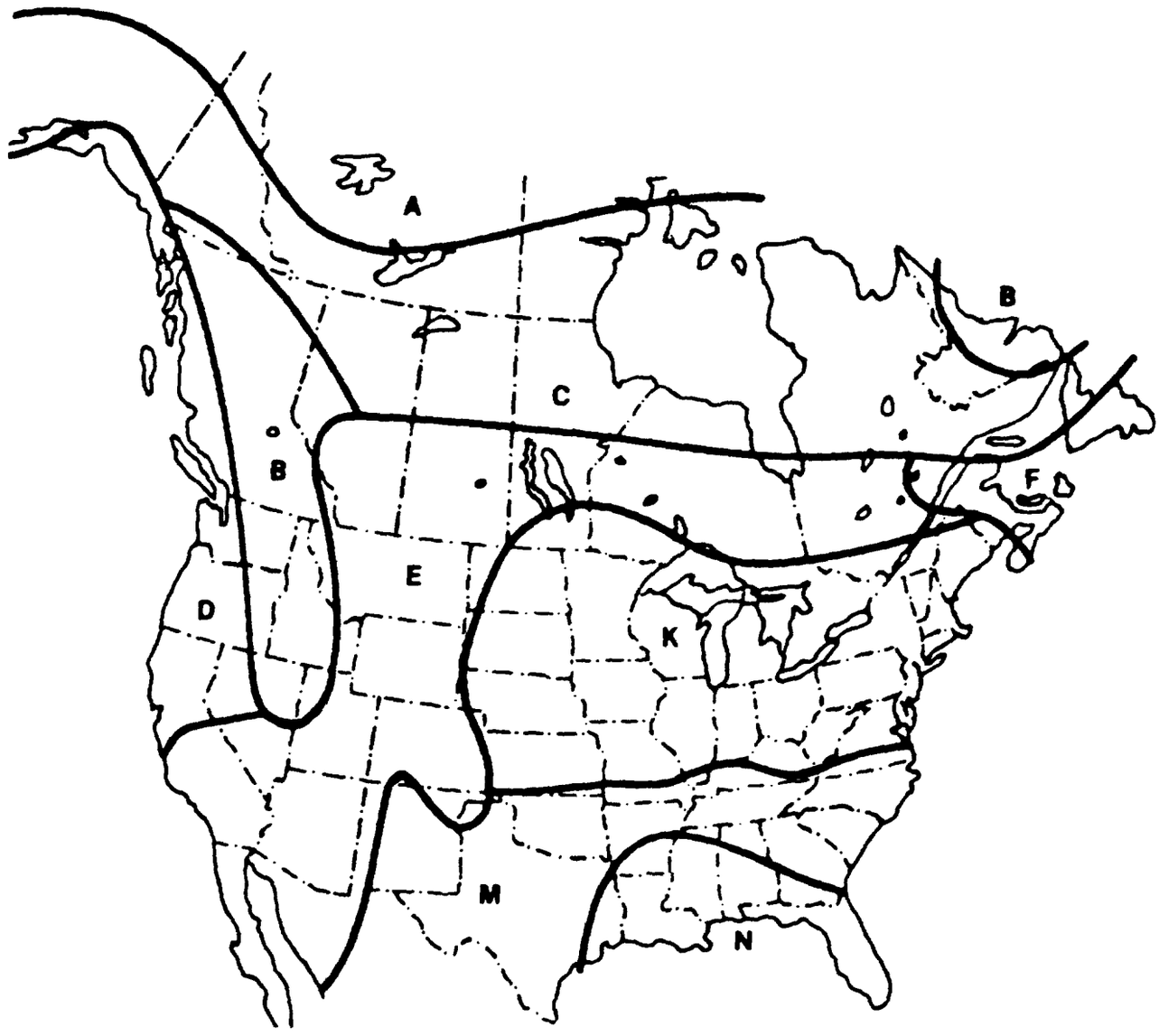

Figure 3.6-2. CCIR Rain Climatic Zones for the Continental United States and Canada

Table 3.6-1. Rainfall Intensity Exceeded (mm/h) for CCIR Rain Climatic Zones

% Time	A	B	C	D	E	F	G	H	J	K	L	M	N	P
1.0	<0.5	1	2	3	1	2	3	2	8	2	2	4	5	12
0.3	1	2	3	5	3	4	7	4	13	6	7	11	15	34
0.1	2	3	5	8	6	8	12	10	20	12	15	22	35	65
0.03	5	6	9	13	12	15	20	18	28	23	33	40	65	105
0.01	8	12	15	19	22	28	30	32	35	42	60	63	95	145
0.003	14	21	26	29	41	54	45	55	45	70	105	95	1409	200
0.001	22	32	42	42	70	78	65	83	55	100	150	120	180	250

The CCIR also provides maps showing isometric rain rate contours for the 0.01 percent exceedance value, which will be used in the attenuation model procedure. This isometric map is given as Figure 3.6-3.

The CCIR model assumes that the horizontal extent of the rain is coincident with the ambient 0°C isotherm height, which will vary with location, season of the year, time of day, etc. An average value of the 0°C isotherm weight is used in the CCIR model, obtained from,

$$h_r = 4.0 \qquad \text{for } 0 < \phi < 36^\circ$$
$$= 4.0 - 0.075\,(\phi - 36) \qquad \text{for } \phi \geq 36^\circ \qquad (3.6\text{-}1)$$

where ϕ is the latitude of the location of interest, in degrees N or S.

This estimate is recognized as having high variability, particularily at higher latitudes, and for locations where the significant rain accumulation occurs at other than the summer rainy season.

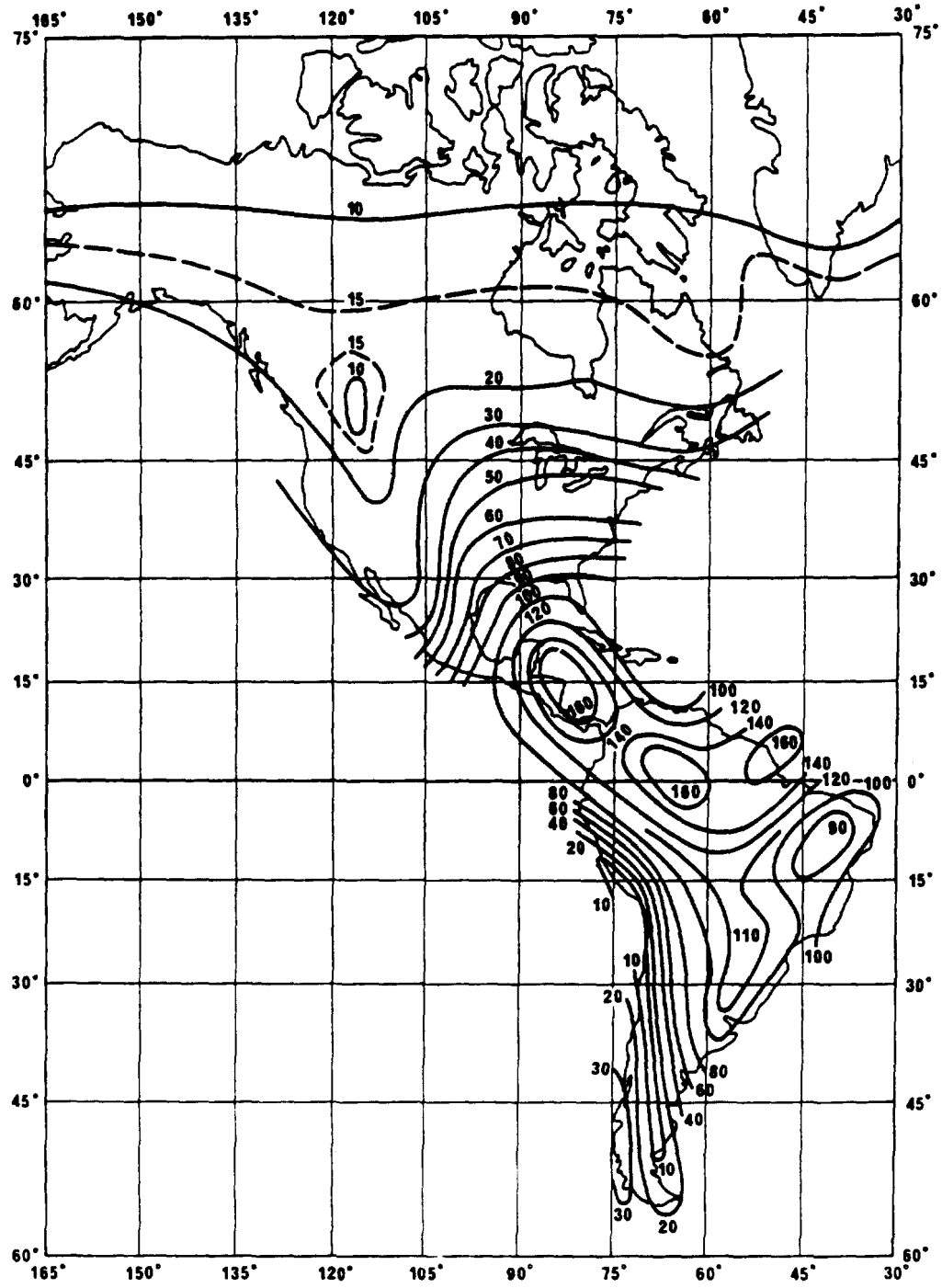

Figure 3.6-3. Contours of Rain Rate Exceeded for 0.01% of the Time (mm/hr) (Sheet 1 of 3)

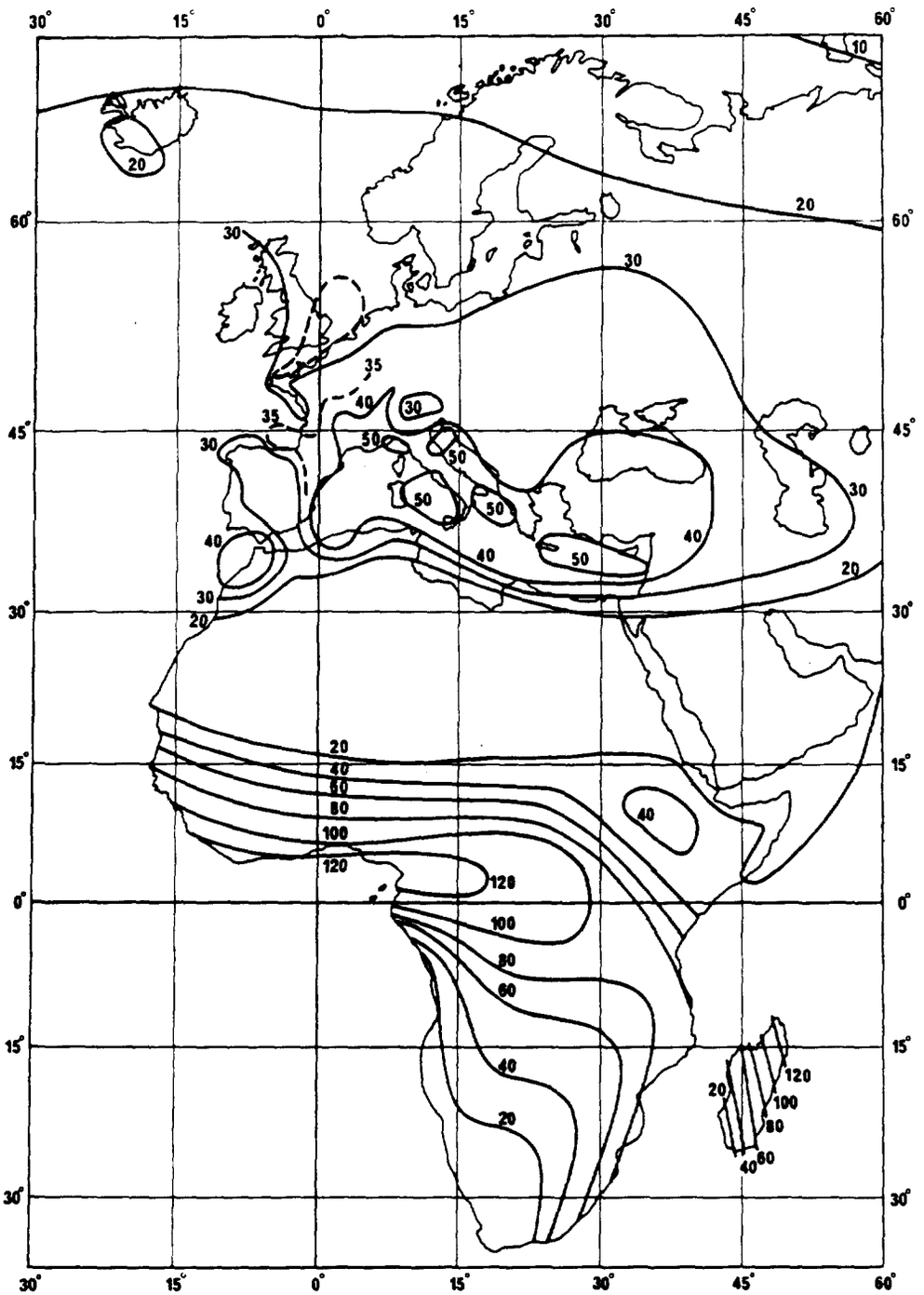

Figure 3.6-3. Contours of Rain Rate Exceeded for 0.01% of the Time (mm/hr) (Sheet 2 of 3)

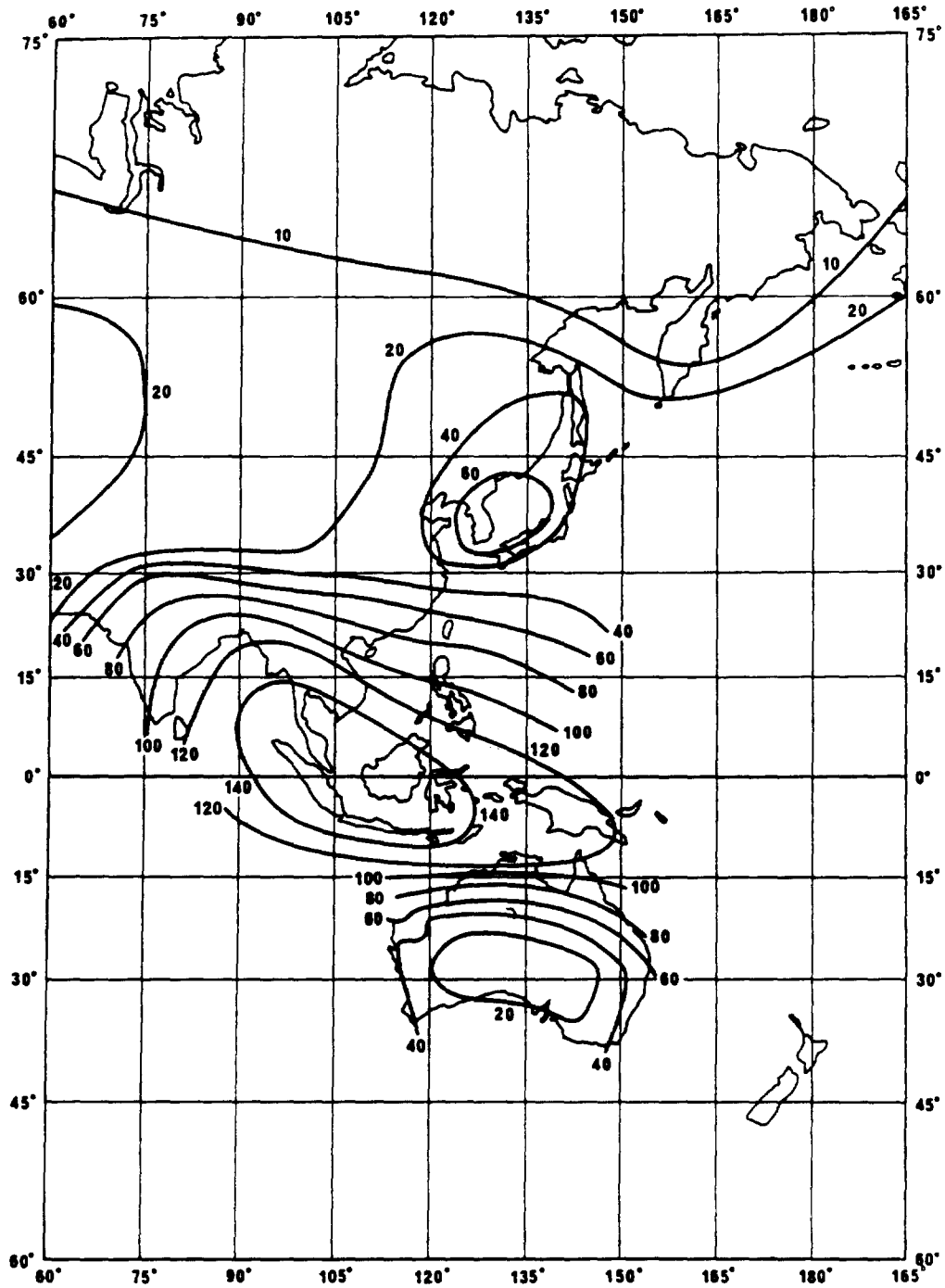

Figure 3.6-3. Contours of Rain Rate Exceeded for 0.01% of the Time (mm/hr) (Sheet 3 of 3)

3.6.2 CCIR Attenuation Model

The CCIR attenuation prediction requires the following input parameters:

- frequency (GHz)
- latitude of earth station (degrees),
- height above mean sea level of earth station (km)
- elevation angle to the satellite (degrees), and
- point rainfall rate for the location for 0.01% of an average year (mm/h.

The rain height, h_r, is determined from the latitude by equation (3.6-1) above. The projected path length on the earth's surface, L_g, and the slant path length through the rain, L_s, are geometrically determined from h_r, the elevation angle, and the height above sea level. A slant path length reduction factor is then applied to account for the horizontal non-uniformity of rain for the 0.01% of the time condition. The reduction factor, r_p, is given by:

$$r_p = \frac{1}{1 + 0.045\ L_g} \qquad (3.6\text{-}2)$$

The product of L_s and r_p is the effective path length through rain for 0.01% of the time.

The specific attenuation for 0.01% of an average year, $\alpha_{0.01}$, in dB/km, is determined from the power-law relationship with rain rate, [see equation (2.3-5)], utilizing the rain rate at 0.01% of the year from locally measured data (preferred), or from Table 3.6-1. The power law coefficients at the frequency and polarization of interest can be obtained from Table 2.3-2, Table 2.3-3, or other

suitable sources. The specific attenuation in the CCIR model is assumed to be constant up to the rain height.

The attenuation exceeded for 0.01% of an average year is then obtained from,

$$A_{0.01} = \alpha_{0.01} L_s r_p \text{ dB} \qquad (3.6\text{-}3)$$

The attenuation exceeded for other percentages of an average year, p, in the range 0.001% to 1%, are then determined from $A_{0.01}$ by,

$$A_p = 0.12 A_{0.01} p^{-(0.546 + 0.043 \log p)} \text{ dB} \qquad (3.6\text{-}4)$$

The CCIR reports that when the above prediction method was tested with measured data for latitudes above 30°, the prediction was found to be in agreement at the 0.01% point to within 10%, with a standard deviation of 30%, when used with simultaneous rain rate measurements. Between latitudes of 20° and 30° the prediction method consistently over-estimated the attenuation by a factor of about one-third. When local measured rain rate statistics are used instead of the average year values given in the CCIR climatic zone tables, the errors are found in general to be less, at all latitudes (CCIR-1986a).

The detailed step-by-step procedure for the CCIR attenuation prediction model, including an example application, is presented in Section 6.3 of the handbook.

3.7 THE LIN MODEL

3.7.1 Empirical Formulas

The set of empirical formulas presented here for earth-satellite path attenuation is an extension of those obtained previously for terrestrial microwave radio paths (Lin-1978). In the case of terrestrial paths, the calculation of the expected rain attenuation

distribution from a long term (20 years) distribution of 5-minute point rain rates has been accomplished using empirical formulas deduced from available rain rate and rain attenuation data measured on nine 11 GHz radio paths (5-43 km) at five different U.S. locations (Lin-1977).

These empirical formulas for terrestrial paths, are (Lin's notation (1978) reverses the role of α and β)

$$\alpha(R) = a\ R^b \text{ dB/km} \tag{3.7-1}$$

$$\beta(R,L) = \alpha(R)\ L \left[1 + \frac{1}{\bar{L}(R)}\right]^{-1} \text{ dB} \tag{3.7-2}$$

where

$$\bar{L}(R) \approx \frac{2636}{R - 6.2} \text{ km} \tag{3.7-3}$$

R is the 5-minute point rain rate in mm/h, L is the radio path length in km, β(R,L) is the path rain attenuation in dB at the same probability level as that of R, and the parameters a and b are functions (Setzer-1970, Chu-1974, Saleh-1978) of the radio frequency, as shown in Figure 3.7-1. (Strictly speaking, the parameters a and b are also functions of wave polarization.)

3.7.2 Rain Path Averaging

If the rain rates were uniform over a radio path of length L, the path rain attenuation β(R,L) would be simply α(R). L, representing a linear relationship between β and L. However, actual rainfalls are not uniform over the entire radio path, and therefore the increase of β(R,L) with L is nonlinear.

Two factors in the empirical method account for the radio path averaging effect. First, the method is based upon the long term distribution of 5-minute point rain rates in which the 5-minute time averaging partially accounts for the fact that the radio path performs a spatial averaging of non-uniform rain rates (Freeny and Gabbe-1969, Drufuca and Zawadzki-1973, Bussey-1950). A 5-minute average of the rain rate seen at a point corresponds to spatially averaging approximately 2.1 km of vertically variable rain rates, assuming 7 meters/second average descent velocity of rain drops.

Figure 3.7-2 shows how the point rain rate distribution, from two years of measurements at Palmetto, Georgia, depends on the average time intervals (range: 0.5-60 minutes). The probability of a 5-minute rain rate exceeding the 40 mm/h threshold is 1/2 that of a 0.5-minute rain rate exceeding the same threshold. From another viewpoint, increasing the averaging time interval from 0.5 to 5 minutes reduces the 0.01 percentile (i.e., 53 minutes/year) rain rate from 87 to 58 mm/h.

However, since most radio paths of interest are longer than 2.1 km, the fixed 5-minute average interval cannot adequately account for all the path length variations. This deficiency is compensated for by the factor

$$\left[1 + \frac{1}{\bar{L}(R)}\right]^{-1} \qquad (3.7\text{-}4)$$

In other words, the auxiliary nonlinear factor represents the empirical ratio between the 5-minute point rain rate R and the radio path average rain rate $R_{av}(L)$ at the same probability level. Since the significant difference between the 5-minute point rain rate and the 0.5-minute point rain rate in Figure 3.7-2 already accounts for the major portion of the difference between the radio path average rain rate $R_{av}(L)$ and the 0.5-minute point rain rate, the auxiliary factor is a weak nonlinear function of L. Obviously, many different analytic functions can be used to approximate this mildly nonlinear

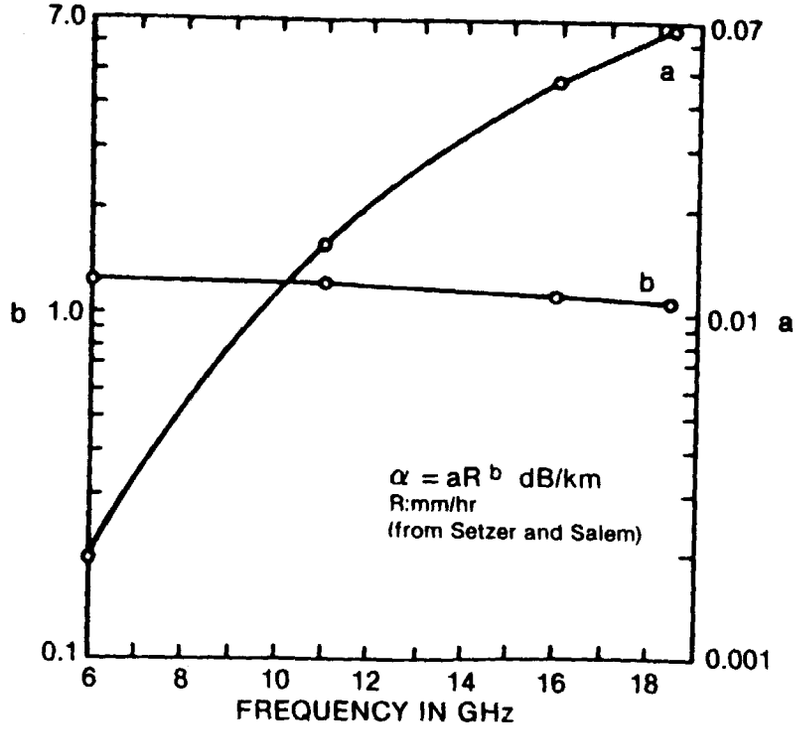

Figure 3.7-1. Dependence of Parameters a and b on the Radio Frequency

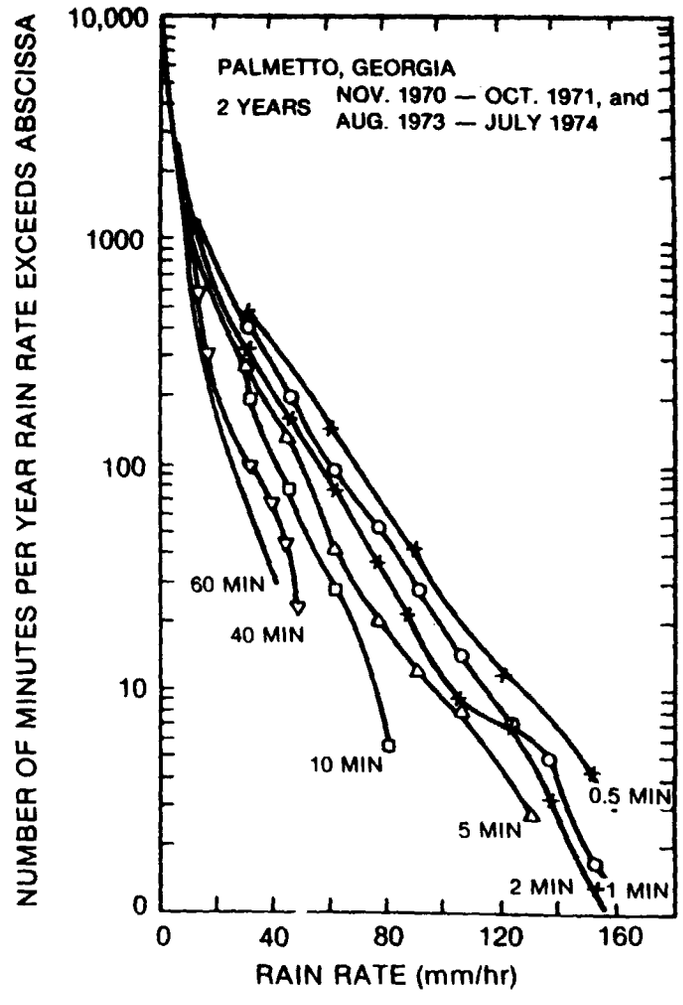

Figure 3.7-2. Dependence of Rain Rate Distribution on Tipping Bucket Rain Gauge Integration Time From Two Years of Measurement at Palmetto, Georgia

behavior. The single parameter function is selected for its simplicity. The adequacy of this simple approximation is supported by the rain rate and rain attenuation data measured on nine, 11-GHz, terrestrial radio paths at five U.S. locations (Lin-1977).

3.7.3 Earth-Satellite Path Legend

To extend the method to earth-satellite paths, let H be the long-term average height of the freezing level in the atmosphere, measured relative to sea level. The effective average length of the earth-satellite path affected by rain is then

$$L = (H - H_g)/\sin\theta \qquad (3.7\text{-}5)$$

where θ is the satellite elevation angle as viewed from the earth station, and H_g is the ground elevation measured from the sea level. The radar measurements of rainfall reflectivity at Wallops Island, Virginia indicate that on the average rainy day (CCIR-1977)

$$H \approx 4 \text{ km} \qquad (3.7\text{-}6)$$

Thus given the elevation angle θ, the ground elevation H_g and the distribution of 5-minute point rain rates, we can calculate the rain attenuation distribution on the earth-satellite path through the use of equations 3.7-1, 2 and 5.

Notice that equation 3.7-5 implies that the path rain attenuation (R,L) varies exactly as the cosecant of the elevation angle θ with this simple extension of the terrestrial model. Also note that these simple formulas are valid only on the long term average. The short term relationships between the surface point rain rate and the earth-satellite path rain attenuation, on a storm-by-storm basis, have been observed to be erratic and difficult to predict.

3.8 THE SIMPLE ATTENUATION MODEL (SAM)

The Virginia Polytechnic Institute and State University (VPI&SU), Blacksburg, VA, has been engaged for several years in the

development of rain attenuation models and related measurement programs. Several iterations of a quasi-physical model of rain attenuation on a slant path have been provided. One of the earliest versions of a comprehensive rain attenuation prediction model was the Piecewise Uniform Rain Rate Model, (Persinger, et al-1980) [described in detail in the previous (3rd) edition of this handbook]. The Piecewise Uniform Model accounted for the nonuniform spatial characteristics of rain with two simplifying assumptions: a) the spatial rain rate distribution is uniform for low rain rates, and b) as peak rain rate increases, the rain rate distribution becomes increasingly nonuniform.

The Piecewise Uniform Model was later extended with an expanded global data base to an exponential shaped rain rate profile (Stutzman and Dishman - 1982, 1984), and was called the Simple Attenuation Model (SAM). The model was further modified to include the effects of rain depolarization and an even larger data base (Stutzman and Yon, 1986). This latest version of the SAM will be described here.

The SAM is a semiempirical model that describes the spatial rainfall along a slant path ℓ by:

$$R(\ell) = R_o \qquad R_o \leq 10 \text{ mm/h}$$

$$= R_o \exp[-\lambda \ln(R_o/10) \quad \ell\cos\beta \qquad R_o > 10 \text{ mm/h} \tag{3.8-1}$$

where

$$\ell \leq L, \qquad L = (H_e - H_o)/\sin\beta \tag{3.8-2}$$

and

R_o is the point rainfall rate in mm/h,
H_o is the earth station altitude in km,
H_e is the effective rain height in km,
β is the slant path elevation angle, and
λ is an empiricaly developed parameter
controlling the rate of decay of the horizontal profile.

The effective rain height is approximated by

$$H_e = H_i \qquad R_o \leq 10 \text{ mm/h} \qquad (3.8\text{-}3)$$

$$= H_i + \log(R_o/10) \qquad R_o > 10 \text{ mm/H}$$

where H_i is the 0°C isotherm height in km. The seasonal average is obtained from (Crane-1978),

$$H_i = 4.8 \qquad \varepsilon \leq 30°$$

$$= 7.8 - 0.1\varepsilon \qquad \varepsilon > 30° \qquad (3.8\text{-}4)$$

here ε is the station latitude, in degrees N or S.

The total attenuation due to a point rainfall rate R_o is found by integrating Eq (3.8-1) over the path L:

$$A(R_o) = aR_o^b L \qquad R_o \leq 10 \text{ mm/h} \qquad (3.8\text{-}5)$$

$$A(R_o) = aR_o^b \frac{1 - \exp\left[-b\lambda \ln(R_o/10)\, L \cos\beta\right]}{b\lambda \ln(R_o/10) \cos\beta}$$

$$R_o > 10 \text{ mm/h}$$

An evaluation of 36 data sets in the expanded VPI&SU data base for which both attenuation and rain rate data were available found that a value of

$$\lambda = 1/14 \qquad (3.8\text{-}6)$$

gave the best fit to the data. The functional dependence of λ is such that large changes do not produce changes in attenuation.

The revised SAM model was found by its authors to give equal to or slightly better predictions than the CCIR or the Global prediction models, for the available data base (Stutzman and Yon - 1986). Figure 3.8-1 shows a comparison of the models for 64 global data sets. Predictions are based on rain rates calculated from the CCIR rain rate model except for the Global Model which uses the Global rain rate model. Mean deviation and standard deviation of predicted attenuation as a percent based on measured attenuation are shown. Figure 3.8-2 shows a similar comparison for 31 long term

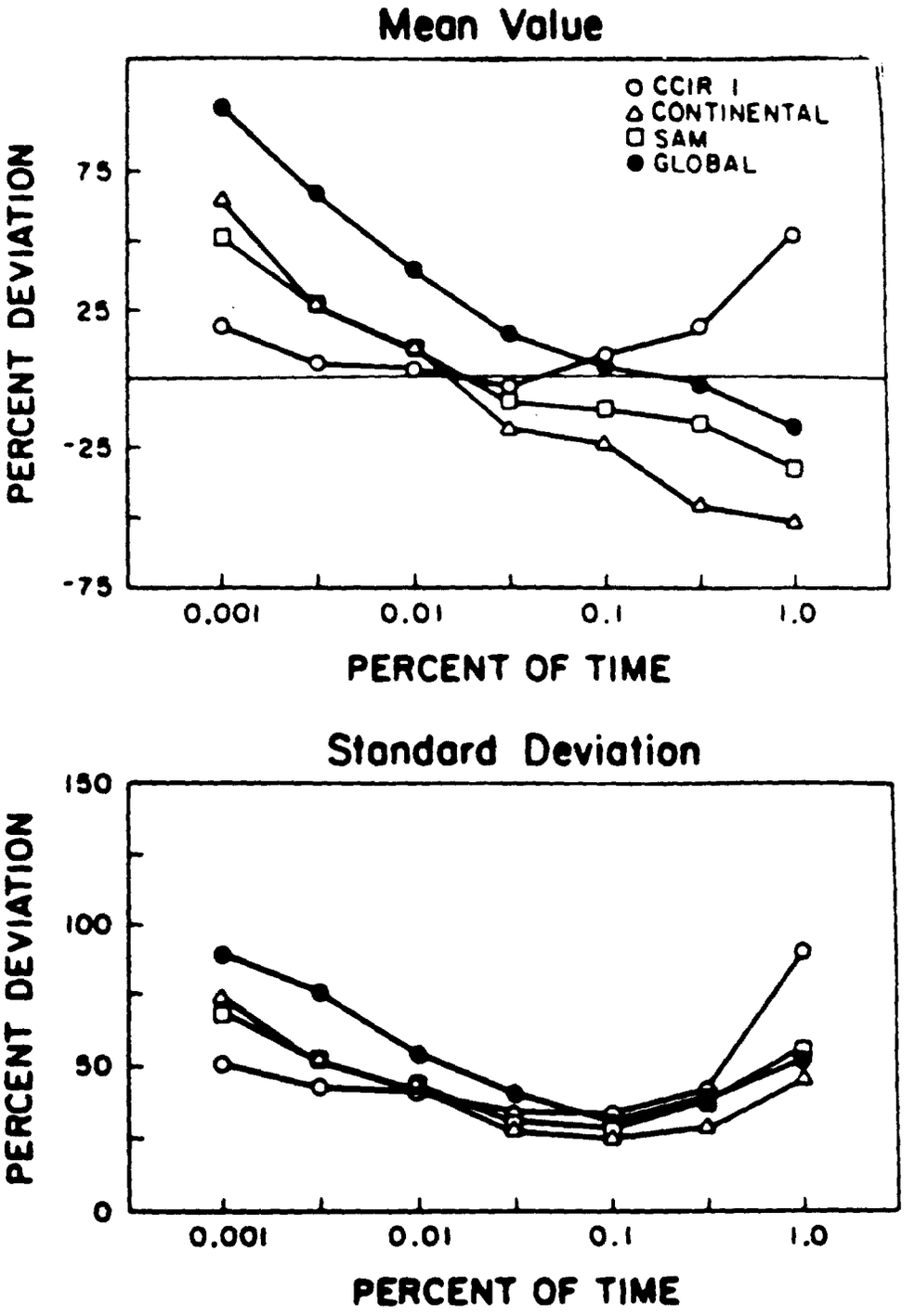

Figure 3.8-1. Comparison of the SAM model with the CCIR and Global models, for 62 measured data sets

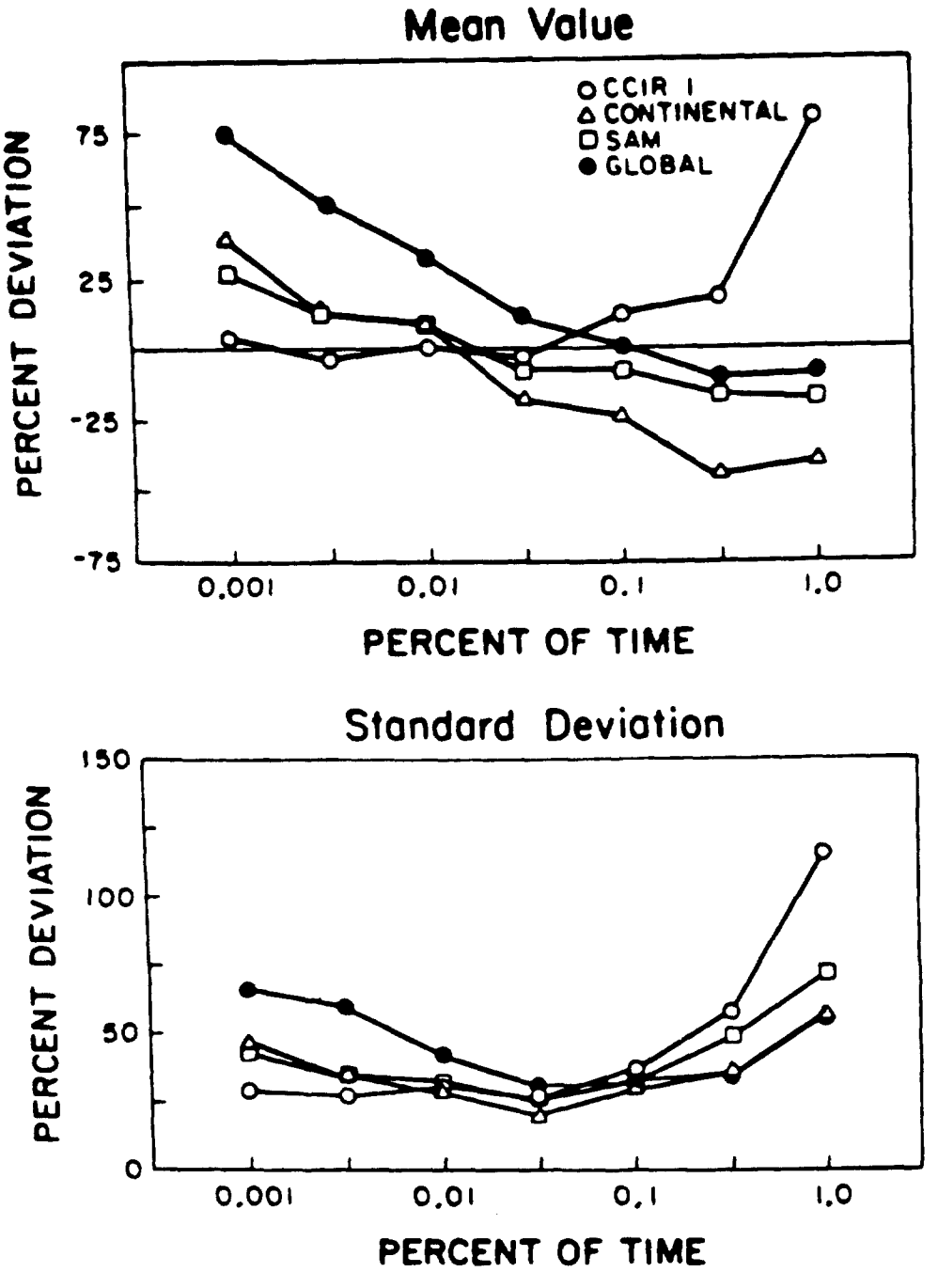

Figure 3.8-2. Comparison of the SAM model with the CCIR and Global models, for 32 long term (two years or more) measured data sets

(two years or more) data sets from the data base. All four models give better predictions for long term data sets, as expected, since they are more representative of average rain behavior, for which the models are based.

3.9 THE EFFECTIVE PATH LENGTH CONCEPT

3.9.1 Definition of Effective Path Length

The effective path length L_e is usually defined as that parameter which relates the specific attenuation to the total attenuation along the earth-space path. Mathematically it is written

$$A = aR^bL_e \qquad (3.9\text{-}1)$$

Alternatively, L_e is the hypothetical path length of uniform rain rate R which will produce the same total path attenuation as the real varying rain rate does along the path. The form of L_e and the technique employed for its derivation has been quite variable. For example, in some cases it is termed effective path length and in others the path averaging factor.

Since rains are not usually uniform over the extent of the storm (rain cells of higher rain rates are small compared to the extent of the storm), the total attenuation is

$$A = \int_0^L \alpha_1 \, d\ell \qquad (3.9\text{-}2)$$

where A is the total attenuation at a given frequency and time through the storm of extent L along the path ℓ. The factor α_1 is a "high resolution" specific attenuation depending on the rain rate at each point along the path. The effective path length in kilometers

$$L_e = \frac{A}{\alpha_{avg}} \qquad (3.9\text{-}3)$$

is where α_{avg} is an analytically determined attenuation per kilometer assuming a uniform average rain rate. The average rain rate is based on rain rate measurements taken over a long period of time. The measured attenuation is also indirectly a function of average rain rate. Measured attenuation and measured rain rate data are compared on an equal probability of occurrence basis over a long time base. This removes the instantaneous time dependence of the measurements. Note that if rain rate is not a function of length ℓ, then $A = \alpha_{avg}L$ and the effective path length would equal the physical rain extent L. This is one limit which occurs for low rain rates. For example, for stratiform rains the rain rate is nearly spatially uniform.

3.9.2 Frequency Dependence of Effective Path Length

Some frequency dependence to the effective path length has been observed at higher rain rates. To investigate the frequency dependence of L_e consider the ratio of two L_e's for two frequencies f_1 and f_2. Namely,

$$\frac{L_e(f_1)}{L_e(f_2)} = \frac{\alpha_{avg}(f_2)}{\alpha_{avg}(f_1)} \frac{\int_0^L \alpha_1(f_1)\, d\ell}{\int_0^L \alpha_1(f_2)\, d\ell} = r_p r_m^{-1} \qquad (3.9\text{-}4)$$

where r_m is the ratio of the measured attenuations, and r_p is the ratio of the predicted attenuations assuming uniform rain conditions, which is also the ratio of predicted specific attenuations. For the effective path length to be independent of frequency r_m must equal r_p and the effective path length versus rain rate must be identical for the two frequencies. Experimental results shown in Figure 3.9-1 demonstrate that for two frequencies

(19 and 28 GHz) and rain rates exceeding one inch per hour the effective path length of the higher frequency is as much as 20% longer than the lower frequency. This is an effect which must be considered when frequency scaling attenuation measurements over a wide frequency range.

The frequency dependence of effective path length shown in Figure 3.9-1 arises from the nonuniformity of rain along the propagation path in combination with the nonlinear dependence of the specific attenuation on rain rate. Using the definition in equation 3.9-1, the relation (Kheirallah, et al-1980)

$$L_e(f_2) = L_e(f_1)^{b(f_2)/b(f_1)} \qquad (3.9\text{-}5)$$

has been derived. This relation has been compared with some experimental data and appears to apply best to the low frequency (4 to 10 GHz) data for high rain rates (exceeding 25 mm/h). Kheirallah, et al (1980) attributes this to the relatively significant effects of cloud attenuation at higher frequencies and low rain rates.

Rewriting equation 3.9-5 one has

$$[L_e(f_1)]^{1/b(f_1)} = [L_e(f_2)]^{1/b(f_2)} = L_e' \qquad (3.9\text{-}6)$$

L_e' is defined as the normalized effective path length and is much less dependent on frequency than L_e. Kheirallah, et al (1980) suggests that for small percentages of time for which rain attenuation dominates, data sets should be expressed in terms of L_e' before data at various frequencies and elevation angles are combined.

3.9.3 Effective Path Length Versus Measurement Period

Experimentally determined effective path lengths for varying measurement periods (such as annual and worst month) show a high variability. For example, in Figure 3.9-2 each curve was developed from equal probability attenuation - rain rate measurements for the

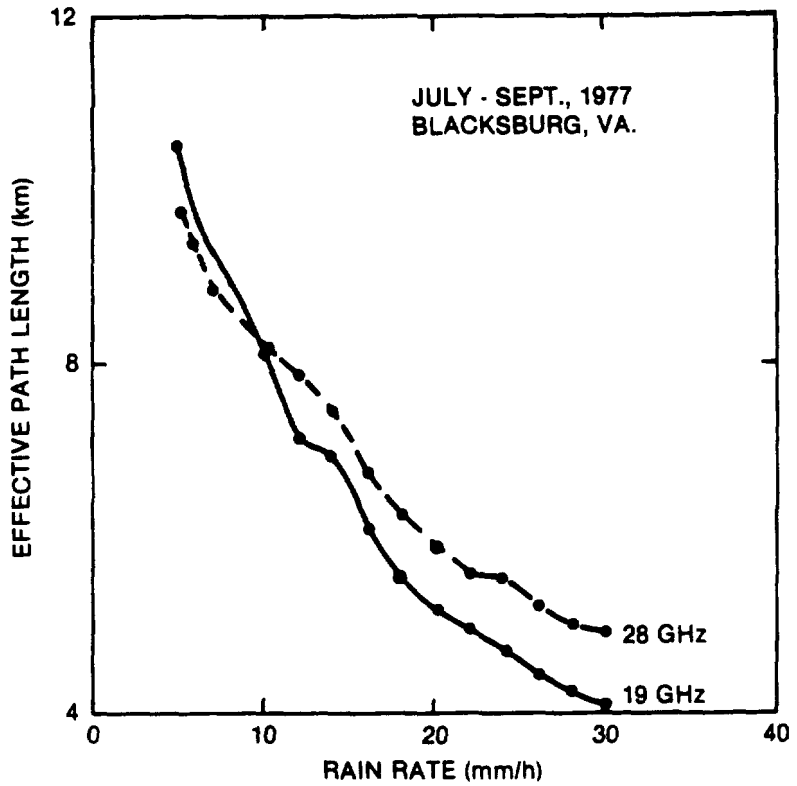

Figure 3.9-1. Effective Path Lengths for the VPI & SU COMSTAR 19 and 28 GHz Systems

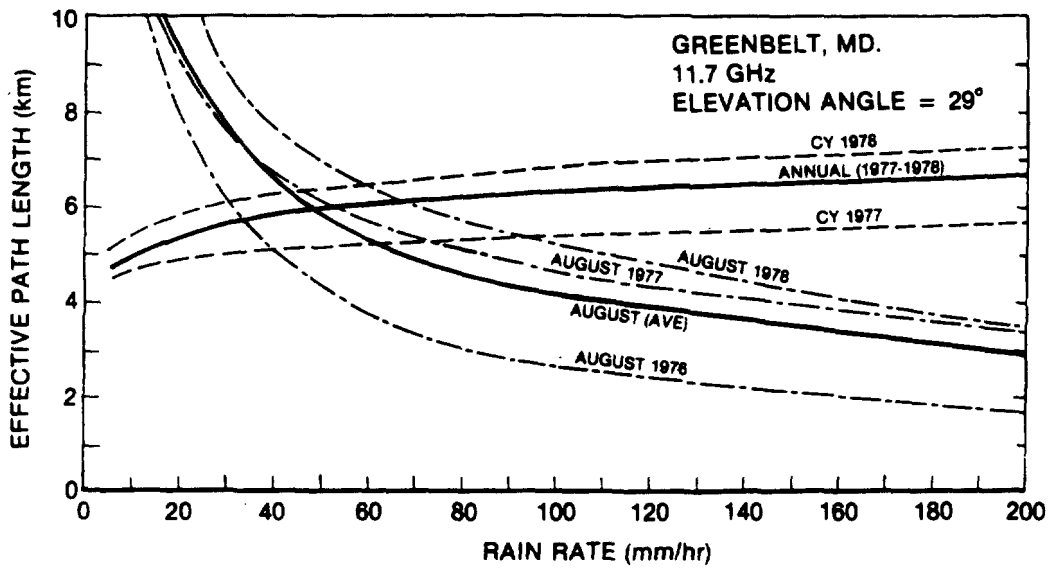

Figure 3.9-2. Effective Path Length for Annual & Worst Month Periods

period indicated. Two trends are apparent. First, the monthly curves show a decreasing path length with increasing rain rate, and second, the annual curves show a path length which increases slightly with rain rate. The first effect arises because the high rain rate events in August are primarily convective storms with intense localized rain rates. The second effect is probably accounted for because the winter rains in Maryland are more uniform in nature and the zero degree isotherm is significantly lower in winter. For this case L_e approaches L for cold weather low rain rate events. However, this effect has not always been observed (see below) and probably indicates that regions with low rainfall during the cold weather months will show a rain rate dependence to L_e similar to that for the worst month.

3.9.4 Comparison of Effective Length Factors

Several of the attenuation models utilize a factor easily related to L_e. It is of interest to compare these factors and determine their relative differences based on a similar set of assumptions. First consider the L_e factor in each model separately.

3.9.4.1 Dutton-Dougherty Model. This model does not explicitly employ an effective path length. An effective path length may be evaluated, however, and it has been by Dutton, et al (1982) for the purpose of comparison with the Global model. The relation between the effective path length given by the DD Model and the rain rate is a complex one, being determined by the liquid water content versus height function, L(h), and the probability modification factor, F. There are two choices for L(h), corresponding to stratiform and convective rain, and the model combines these for some time percentage values. Because a simple expression for L_e is not possible, no attempt is made here to define an effective path length for this model.